

Chaoyang Xie

School of Mechatronics Engineering,
University of Electronic Science and
Technology of China,
Chengdu 610054, China;
Institution of System Engineering,
China Academy of Engineering Physics,
Mianyang 621999, China

Pingfeng Wang¹

Department of Industrial and
Manufacturing Engineering,
Wichita State University,
Wichita, KS 67260
e-mail: pingfeng.wang@wichita.edu

Zejun Wang

Department of Industrial and
Manufacturing Engineering,
Wichita State University,
Wichita, KS 67260

Hongzhong Huang

School of Mechatronics Engineering,
University of Electronic Science and
Technology of China,
Chengdu 610054, China

Corrosion Reliability Analysis Considering the Coupled Effect of Mechanical Stresses

Corrosion is one of the most critical failure mechanisms for engineering structures and systems, as corrosion damages grow with the increase of service time, thus diminish system reliability gradually. Despite tremendous efforts, effectively carrying out reliability analysis considering the complicated coupling effects for corrosion remains to be a grand challenge. There is a substantial need to develop sophisticated corrosion reliability models and effective reliability analysis approaches considering corrosion damage growth under coupled effects such as mechanical stresses. This paper presents a physics-of-failure model for pitting corrosion with the coupled effect of corrosion environment and mechanical stresses. With the developed model, corrosion damage growth can be projected and corrosion reliability can be analyzed. To carry out corrosion reliability analysis, the developed pitting corrosion model can be formulated as time-dependent limit state functions considering pit to crack transition, crack growth, and fracture failure mechanics. A newly developed maximum confidence enhancement (MCE)-based sequential sampling approach is then employed to improve the efficiency of corrosion reliability analysis with the time-dependent limit state functions. A case study is presented to illustrate the efficacy of the developed physics-of-failure model for corrosion considering the coupled mechanical stress effects, and the new corrosion reliability analysis methodology. [DOI: 10.1115/1.4032003]

Keywords: pitting corrosion, reliability, physics-of-failure, adaptive sampling

1 Introduction

For engineering systems, especially metallic structures, corrosion has been recognized as one of the most important degradation mechanisms that affect the long-term reliability and integrity [1]. Different corrosion environments could cause several kinds of defects on structures, such as pitting corrosion, uniform corrosion, hydrogen embrittlement, and crevice corrosion [2–4]. Corrosion damages may result in catastrophic system hazards in health management and long-term safety services in many industries. For example, in oil industries, metallic pipes are commonly made from steel and iron, and the corrosion damages could lead to oil leaks in pipelines, and further unplanned maintenance and plant unavailability. In nuclear energy industry, the alloy structure used in nuclear reactors may corrode in radioactive, high-temperature, and high-pressure environments. For aircrafts, the corrosion pits on the surface and corrosion fatigue cracks that are hidden inside the fuselage joints serve as one of the main causes for failures of aged aircrafts. With the growth of the pit due to corrosion, it can transform to a crack, leading to fatigue failures when subjected to stress loads and becomes very critical for structure safety service. Thus, the development of effective reliability prediction technologies for pitting corrosion damages is essential for facilitating maintenance decision-making and successful prevention of catastrophic structural failures.

Tremendous research efforts have been undertaken in the past decade to model the corrosion process and develop corrosion reliability analysis methods [5–9]. To analyze the corrosion reliability, the pitting corrosion damage is usually extrapolated to future times using various empirical models based on experimental data, in which the models used generally present the relationship between

the pitting depth and the corrosion time. Representative corrosion models include the power function model, the Paik linear model [10], and the Melchers nonlinear multistage model [11]. Qin et al. [12] compared these corrosion models and proposed a probabilistic corrosion model based on the Weibull function for hull structure analysis. Melchers [13] assumed that the maximum depth of pitting corrosion follows the extreme value distribution, and further proposed a model to present the carbon steel corrosion depth in immersion environment. In addition, the average corrosion depth has also been used as a key parameter for some corrosion assessment models. The study conducted by Shao et al. [14] focused on the corrosion failure of buried pipelines considering the combined effects of external loads and corrosion, in which the longitudinal and circumferential force characteristics were taken into account in the failure model. The study results showed that the internal pressure, residual stress, wall thickness, yield strength, and the environmental condition are all important factors contributing to pipeline corrosion failures. Despite the deterministic corrosion models reported in the literature, some scholars have also considered corrosion as a random process, and consequently stochastic-process-based approaches, such as the Markov chains, have been used for the modeling of pitting corrosion [15–18]. In the study conducted by Provan and Rodriguez, a nonhomogenous Markov process has been employed to model pitting growth [17]. Valor [18] also proposed a stochastic corrosion model in which the pit initiation was considered as a Weibull process and the pit growth was modeled by a nonhomogenous Markov process. Zhang et al. [19] used the same stochastic models to investigate the pitting corrosion susceptibility of pure Mg and Mg alloys.

Besides the empirical models based on experimental data, another type of method for corrosion reliability analysis is based on physics-of-failures, in which the corrosion damage is described by electrochemical and mechanical processes [20–26]. The physics-of-failure is an approach that utilizes knowledge of the relationships

¹Corresponding author.

Manuscript received March 4, 2015; final manuscript received November 7, 2015; published online July 1, 2016. Assoc. Editor: Sankaran Mahadevan.

between requirements and the physical characteristics of the product, including the reaction of product elements and materials to loads (stressors) and interaction under loads. Hoepfner and Arriscorreta [2] developed a seven-stage conceptual model for corrosion fatigue, in which the electrochemical effects in pit formation and the role of pitting in fatigue and corrosion-induced fatigue crack nucleation behavior were considered. Shi and Mahadevan [22] developed a computational implementation approach based on the seven-stage conceptual model for corrosion fatigue life prediction. Other than the seven-stage model, Harlow and Wei [21] proposed a three-stage probabilistic model, in which the crack initiation, surface cracks grow through a crack, and the crack fracture were considered as three distinct stages for corrosion failures. Although the operating stage loading conditions have been considered in the studies aforementioned, all the models developed in the literature have been focused on structures with cyclic loadings and the initial preloaded stress effect has not been studied in the pit-growth phase. However, stress corrosion crack (SCC) is another important failure mode, especially for structures with static loads. Although Wu [23] proposed a probabilistic-mechanistic approach focused on modeling SCC propagation of Alloy 600 SG tubes with uncertainties; the pit-growth process considering the stress effects was omitted in the model. Considering the pitting growth to fatigue crack, a transition model for pitting to corrosion fatigue crack nucleation was first proposed by Kondo [24], and further discussed by Chen and Wei [26]. Although this physics-of-failure-based transition model combined the stress effect for reliability analysis at the transition process from pitting to a crack nucleation, the stress effect at the pitting growth stage has not been taken into account in the model, which would lead to substantial error in estimating the corrosion reliability. Because of the complexity of underlying physics for corrosion coupled with stress effects, existing corrosion models have been mainly focused on the corrosion process itself while the mechanical stress impacts to the pit growth have been largely ignored. There is a significant need in corrosion research for the development of a better understanding of corrosion mechanisms, while considering the coupling effects of mechanical stresses and further high-fidelity modeling techniques for the prediction of pitting corrosion reliability.

Despite the modeling of corrosion process, effective reliability analysis approaches based on corrosion models also play an important role for corrosion reliability assessment. In the structure reliability analysis literature, the Monte Carlo simulation (MCS) method has been commonly used as a reliability analysis tool to estimate reliability by evaluating a large number of simulation samples. If sufficient simulations are used, a relatively accurate reliability estimation result can be obtained with a high level of confidence. However, this method is inefficient for many engineering problems, where computationally expensive performance functions are involved [27]. To improve the performance of reliability analysis, various methods, including both analytical- and simulation-based approaches, have been developed. Some representatives include the most probable point (MPP)-based methods [28–32], dimension reduction method (DRM) [33–35], polynomial chaos expansion (PCE) [36–38], and Kriging-based methods [39]. The MPP-based approaches such as the first- or second-order reliability method (FORM/SORM) are to locate the MPP in the U-space and approximate reliability by calculating the reliability index, which is the distance between MPP and the origin in the U-space. However, the MPP-based methods may encounter convergence problems in some cases as reported in the literature [32], and the accuracy might also be sacrificed due to the high nonlinearity of the limit states. The DRM uses an additive decomposition of a response that can simplify a single multidimensional integration for reliability analysis to multiple one-dimensional integrations, and then estimates reliability based on statistical moments of system responses. Recently, the eigenvector DRM has been proposed to enhance the numerical efficiency and stability of the DRM method by incorporating the eigenvector sampling and stepwise moving least-squares techniques. The DRM is shown to be a sensitivity-free method for

reliability analysis; however, the estimation error could be significant for limit state functions with high nonlinearity. The PCE method, which constructs a stochastic response surface approximation with multidimensional polynomials over a sample space of random variables, is one of the methods that could provide more accurate reliability estimations by incorporating more uncertainty samples. While the accuracy of reliability estimation using PCE can be improved by increasing the order of stochastic polynomial terms, the computational cost could be highly prohibited due to the curse of dimensionality: Efficiency of PCE is diminished and computational cost is substantially increased as the number of random variables rises. Other than analytical approaches, surrogate models such as Kriging have also been used widely in reliability analysis and design applications [40–43]. Although this approach takes the advantage of direct MCS for reliability analysis, validation of the Kriging model is still a quite challenging task. In a recent study, an MCE-based sequential sampling approach has been developed for reliability analysis using Kriging surrogate models [44,45]. This approach defines a new measure, referred to as the cumulative confidence level (CCL), to quantify the accuracy of reliability estimation when MCS is used based upon the developed surrogate models. Due to the new adaptive sampling scheme developed in the approach, accurate reliability estimation can be obtained using the MCE-based sampling approach in an efficient manner.

This paper presents a new physics-of-failure-based pitting corrosion reliability model, which considering the coupled effect of corrosion environment and mechanical stresses at the pit-growth stage; thus corrosion damage growth can be projected and corrosion reliability can be analyzed using the developed model. To carry out corrosion reliability analysis, the developed pitting corrosion model can be used to formulate time-dependent limit state functions considering pit to crack transition, crack growth, and fracture failure mechanics. The new MCE-based sequential sampling approach is employed for corrosion reliability analysis with the time-dependent limit state functions to improve the computational efficiency. The rest of this paper is organized as follows: Section 2 briefly reviews the related work in corrosion reliability analysis, focusing on pitting corrosion process modeling and the corrosion reliability analysis using FORM. Section 3 details the developed physics-of-failure model for pitting corrosion damage process, and Sec. 4 presents the MCE-based sequential sampling approach for efficient structure pitting corrosion reliability analysis. One case study is used to demonstrate the efficacy of the developed reliability analysis approach in Sec. 5.

2 Related Work on Pitting Corrosion Reliability Analysis

This section provides a brief review of existing pitting corrosion model and corrosion reliability analysis approach that have been commonly used in the literature, which will be used later in the case study presented in Sec. 5 for the comparison purpose. Section 2.1 discusses the mechanistic model for pitting growth in pitting corrosion modeling, whereas Sec. 2.2 introduces the FORM for corrosion reliability analysis.

2.1 Mechanistic Model for Pit Growth. Pitting corrosion is a localized form of corrosion that occurs when a corrosive medium attacks a metal at specific points causing small holes or pits to be formed. This happens when a protective coating or oxide film is perforated, due to mechanical damage or chemical degradation. The degradation process of pitting corrosion considering the pit growth and crack development from a corrosion pit with a cyclic load, referred to as corrosion-induced fatigue, has been studied in the literature [46–48]. Generally, the pitting corrosion development with a cyclic load can be illustrated by a four-stage process: pit nucleation, pit growth, pit to crack, and crack propagation, as shown in Fig. 1.

Pit nucleation is the first stage in the corrosion damage process, which is highly related to the electrochemical process during

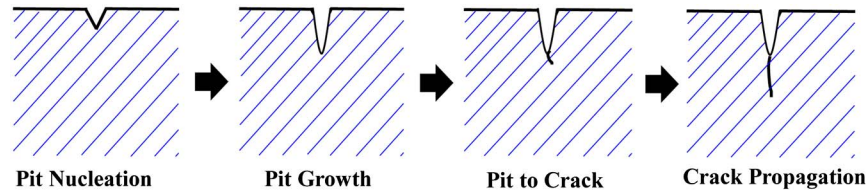


Fig. 1 Pitting corrosion growth and transit to crack process

corrosion. The pit nucleation is a complex process, where the pit initial size and nucleation time largely depend on factors such as loads, materials, corrosion environment, and electrolytes. Due to the complexity, it has been assumed to follow a random process in engineering practice, and accordingly, the initial size of pit has generally been considered as a random variable following a certain statistical distribution, whereas the distribution parameters can usually be obtained with experiment data.

After the nucleation of a pit, the corrosion process enters into the pit-growth stage. A simplified model for pit growth has been developed by Harlow and Wei [21,26]. This developed model assumed that a pit of hemispherical shape grows at a constant volumetric rate in accordance with Faraday's law from an initial radius size, and accordingly, the rate of pit growth is provided as

$$\frac{dV}{dt} = \frac{Mi_0}{zF\rho} \exp\left(-\frac{\Delta H}{RT}\right) \quad (1)$$

where V is the hemispherical pit volume, $V = 2\pi a^3/3$, a is the pit size; M is the molecular weight of the material; i_0 is the pitting current coefficient; z is the valence; F is the Faraday's constant; ρ is the material density; ΔH is the activation energy; R is the gas constant; and T is the absolute temperature.

Based on the model developed by Harlow and Wei, and the pit growth rate provided in Eq. (1), the pit growing depth at a given time, t , can be obtained as

$$a(t) = \left(\frac{3Mi_0}{2\pi zF\rho} \exp\left(-\frac{\Delta H}{RT}\right) * t + a_0^3\right)^{\frac{1}{3}} \quad (2)$$

where a_0 is the initial pit size. However, the activation energy in this model represented the corrosion chemical activation and not considered the stress effect.

With the growth of a pit, a transition from pitting to fatigue crack growth is expected to occur. For corrosion fatigue modeling, this transition will be realized when the effective stress intensity factor for the pit, K_{pit} , exceeds a certain threshold, K_{th} , expressed as

$$K_{\text{pit}} \geq K_{\text{th}} \quad (3)$$

where K_{th} is the threshold of stress intensity factor of crack propagation and K_{pit} is the stress intensity factor for the surface of the pit, which can be obtained as

$$K_{\text{pit}} = \frac{1.12k_t\Delta\sigma\sqrt{\pi a}}{\Phi} \quad (4)$$

where Φ is shape factor and k_t is the stress concentration factor of the pit hole. After a pit is transformed to a crack, the crack propagation stage of the corrosion failure process will begin and the crack size can be modeled based on Paris' law as

$$\frac{da}{dt} = C(\Delta K)^m \quad (5)$$

The crack size development process can be employed from Eq. (1) to Eq. (5), which can be used as a performance response parameter for reliability analysis. Most of the existing corrosion fatigue models consider pitting growth stage without the applied stress. It means that the stress effect has been ignored at the pitting

growth stage, which could lead to significant error in corrosion reliability assessment.

2.2 Corrosion Reliability Analysis Using FORM. Consider a performance model $G(\mathbf{X})$ under the existence of uncertainties, where the system fails if $G(\mathbf{X}) < 0$. If the joint probability density function of random variables \mathbf{X} is $f_{\mathbf{X}}$, the statistical description of a probabilistic performance fails is then completely characterized by the cumulative density function as

$$P_f = \Pr(G < 0) = \int_{G < 0} f_{\mathbf{X}}(\mathbf{X})d\mathbf{X} \quad (6)$$

In practice, the integration boundary $G(\mathbf{X}) = 0$ and the high dimensionality make it difficult or even impossible to obtain an analytical solution to the probability integration in Eq. (6). Simulation and approximation methods are therefore used for reliability analysis. FORM solves the probability integral by simplifying the performance function $G(\mathbf{X})$ using the first-order Taylor series expansion at the MPP. First, transform the original variables \mathbf{X} in \mathbf{X} -space into standard normal variables \mathbf{U} in \mathbf{U} -space, and the performance function is expressed as $G(\mathbf{U})$. Then the reliability index β is obtained by an optimization problem

$$\begin{cases} \min_{\mathbf{U}} & \beta = \|\mathbf{U}\| \\ \text{s.t.} & G(\mathbf{U}) = 0 \end{cases} \quad (7)$$

The probability in Eq. (6) is then computed analytically by the following equation:

$$P_f = \Pr(G < 0) \cong \Phi(-\beta) \quad (8)$$

In summary, current literature for the modeling of the corrosion process has been mainly focused on the relationship between corrosion parameters such as the pit depth and the corrosion environment, while the coupled effect of corrosion environment and mechanical stresses has been largely ignored at the pit-growth stage. In addition to the corrosion process modeling, the FORM has been commonly used as the reliability analysis approach based on a given corrosion model in literature. Although FORM method could provide a relatively good computational efficiency, it would result in large reliability estimation errors, especially when the limit state function is highly nonlinear, since FORM approximates the limit state with a linear function at the MPP. To tackle these challenges, a new physics-of-failure model for pitting corrosion considering the coupled effect of static stress at the pitting growth stage will be presented in Sec. 4, whereas a new MCE-based adaptive sampling approach will be introduced in Sec. 5 for corrosion reliability analysis based on the developed model to improve the efficiency and accuracy.

3 Physics-of-Failure Model for Pitting Corrosion With Coupled Stresses

Based on the electrochemical theory, the electrical current on an electrode depends on the electrode potential. A general representation of the polarization of an electrode is described in the Butler-Volmer equation

$$J = j_0 \exp\left(\frac{zF(\varphi - \varphi_{eq})}{RT}\right) \quad (9)$$

where J is the electrode current density, A/m²; j_0 is the exchange current density, A/m²; φ is the electrode potential, V; and φ_{eq} is the equilibrium potential, V. When the stress is applied on the metal materials with elastic deformation, the equilibrium potential will be varied according to Gutman's theory [47,48]

$$\Delta\varphi_{eq} = -\frac{\Delta PV_m}{zF} \quad (10)$$

where ΔP is the spherical part of macroscopic stress tensor excess pressure (Pa) and V_m is the molar volume of the metal. The current density with the stress effects will be changed as

$$\begin{aligned} J &= j_0 \exp\left(\frac{zF(\varphi - \varphi_{eq} - \Delta\varphi_{eq})}{RT}\right) \\ &= j_0 \exp\left(\frac{zF(\varphi - \varphi_{eq})}{RT}\right) \exp\left(\frac{\Delta PV_m}{RT}\right) \end{aligned} \quad (11)$$

The coefficient, $\exp(\Delta PV_m/RT)$, is used to depict the variance of corrosion current with stress effects compared without stress situation.

In this paper, the effects of stress applied are considered based on Eq. (1), then the corrosion current for a pit with the stress ΔP can be obtained by

$$I_0 = i_0 \exp\left(-\frac{\Delta H}{RT}\right) \exp\left(\frac{V_m \Delta P}{RT}\right) \quad (12)$$

where I_0 is the pitting current; V_m is the molar volume of the material; and ΔP is the bulk component of stress tensor. Thus, taking into account the stress effect in the pit growth, Eq. (1) will be changed as

$$\frac{dV}{dt} = \frac{Mi_0}{zF\rho} \exp\left(-\frac{\Delta H}{RT}\right) \exp\left(\frac{V_m \Delta P}{RT}\right) \quad (13)$$

Accordingly, the pit-growing depth at the time t , as shown in Eq. (2), can be changed to take into account the coupled effects of stress load and corrosion environment as

$$a(t) = \left(\frac{3Mi_0}{2\pi zF\rho} \exp\left(-\frac{\Delta H}{RT}\right) \exp\left(\frac{V_m \Delta P}{RT}\right) * t + a_0^3\right)^{\frac{1}{3}} \quad (14)$$

As the pit depth grows, the stress intensity factor at the pit tip will increase correspondingly, and when it reaches beyond the threshold value of SCC, the pit will transform into a crack and the SCC will thus occur. From the fracture mechanics theory, the thresholds of SCC and the fracture toughness are both material properties, and the relationship between these two thresholds can be expressed by the following equation as [46]:

$$K_{ISCC} = K_{IC} \left(1 - \eta \frac{\rho z F}{\alpha M \sigma_s}\right)^{1/2} \quad (15)$$

where K_{ISCC} is the threshold stress intensity factor of SCC, means the minimum stress required for SCC propagation; K_{IC} is the fracture toughness of the material; η is the anodic polarization potential; α is the coefficient constant; and σ_s is the yield stress.

Similarly, the criteria of a pit transforming into a crack can be obtained based on the thresholds of SCC and the fracture toughness as

$$K_{pit} \geq K_{ISCC} \quad (16)$$

As introduced earlier in Eq. (4), the stress intensity factor for the surface of the pit can be calculated based on the pit shape and stress.

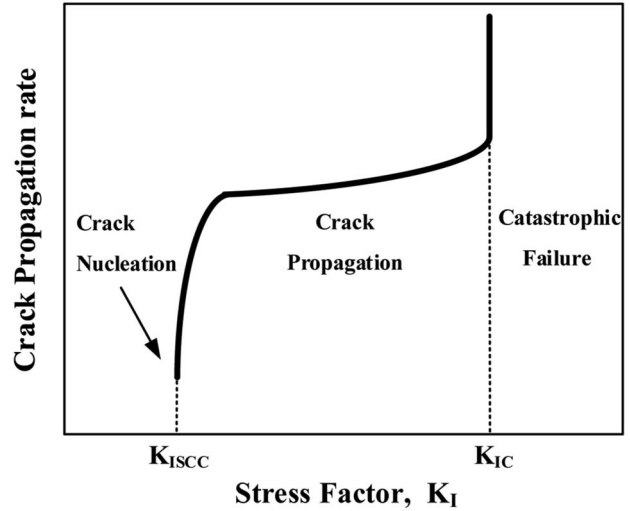


Fig. 2 SCC propagation curve

By letting the threshold of stress intensity factor for SCC as shown in Eq. (12) equal to Eq. (4), the critical size of a pit at the transition to a crack can be calculated as

$$a_{ci} = \frac{1}{\pi} \left(\frac{K_{IC} \Phi}{1.12 k_t \Delta \sigma}\right)^2 \left(1 - \eta \frac{\rho z F}{\alpha M \sigma_s}\right) \quad (17)$$

After the transition from a pit to a crack, the corrosion damage process will turn into the crack propagation stage. Unlike corrosion fatigue crack, which is usually caused by the combination of cyclic load and a corrosive environment, the stress corrosion cracking is generally induced by a static tensile or torsional load to open and sustain the crack. The stress intensity factor at the crack propagation stage is generally a function of the total stress and the crack length. Figure 2 shows a typical crack propagation curve with a threshold stress intensity factor. As shown in the figure, failure due to SCC does not occur until the stress intensity factor reaches K_{ISCC} for a particular material–environment–stress combination. Similarly, the corrosion fatigue failure usually occurs once the stress intensity factor reaches beyond the threshold value K_{IC} .

Following studies reported in Refs. [49–51], in this study, it is also assumed that the empirical model, as shown below, can be used for SCC propagation, which is similar to the fatigue crack propagation modeled by Paris' law

$$\frac{da}{dt} = C(K_I - K_{ISCC})^m \quad (18)$$

where C and m are the model constants of crack propagation. Note that the developed pit-growth model takes into account the coupled effects of corrosion environment and the mechanical stresses at the pit-growth stage of the corrosion damage process. Figure 3 shows two typical pit-growth curves under the same corrosion environment with and without considering the mechanical stress effect, respectively. It can be clearly observed that the coupled stress effect imposes a big impact on the pit-growth process leading to a large growth rate and shorter time until the pit reaches the critical size.

Following the terminology of structure reliability methods and stress–strength interference theory, corrosion failure can generally be defined as the stress intensity factor exceeds the fracture toughness based on fracture mechanics. Accordingly, for corrosion reliability analysis, the corresponding time-dependent limit state function can be written as

$$G(x, t) = K_{IC} - \beta\sigma\sqrt{\pi a(t)} = \begin{cases} K_{IC} - \beta\sigma\sqrt{\pi\left(\frac{3Mi_0}{2\pi z F\rho}\exp\left(-\frac{\Delta H}{RT}\right)\exp\left(\frac{V_m\Delta P}{RT}\right)*t + a_0^3\right)^{\frac{1}{3}}} & \text{(Pit stage)} \\ K_{IC} - \beta\sigma\sqrt{\pi\left(a_{ci} + \int_{t_{ci}}^t C(K_I - K_{ISCC})^m dt\right)} & \text{(Crack stage)} \end{cases} \quad (19)$$

where β is the shape parameter for the crack; σ is the static stress load; $a(t)$ is the pit depth in pitting growth stage or the crack size in crack propagation stage at a given time t . Based on the time-dependent limit state function expressed in Eq. (19), $G(\mathbf{x}, t) > 0$ denotes the safe state, whereas $G(\mathbf{x}, t) < 0$ represents the corrosion failure state. By taking into account the model input uncertainties, Fig. 4 shows the histograms for the limit state function under the same corrosion environment with and without considering the coupled mechanical stress effects, respectively. It is clearly seen from the figure that ignoring the coupled stress effect, an overestimated reliability value will be very much likely obtained, as indicated in the figure that more samples for the limit state function will be larger than zero for the case without considering the coupled stress effect.

As the mechanical stress effect being considered in the developed new pitting corrosion model, an efficient reliability analysis approach is then required to conduct corrosion reliability analysis. In the next section, a new MCE-based adaptive sampling approach will be introduced and employed for corrosion reliability analysis.

4 MCE-Based Adaptive Sampling Approach for Corrosion Reliability Analysis

For corrosion reliability analysis, the performance function $G(\mathbf{x}, t)$ as shown in Eq. (19) will be used and accordingly the probability of corrosion failure can be defined as

$$P_f = P(G(\mathbf{x}, t) \leq 0) = \int \dots \int_{G(\mathbf{x}, t) \leq 0} f_{\mathbf{x}}(\mathbf{x}, t) d\mathbf{x} \quad (20)$$

where the vector \mathbf{x} represents random input variables with a joint probability density function $f_{\mathbf{x}}(\mathbf{x})$, and t denotes time. The reliability $R = 1 - P_f$. It is extremely difficult to evaluate P_f directly using

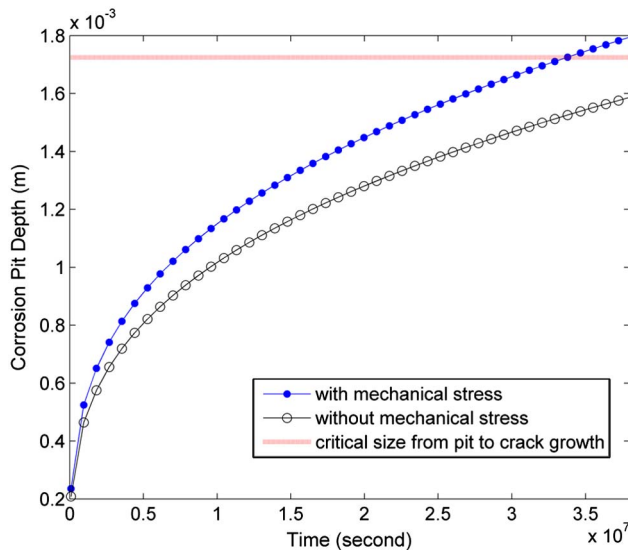


Fig. 3 Comparison of pit growth with and without mechanical stresses

Eq. (20), as it requires numerical evaluation of multidimensional integrations over the failure region. This section introduces a newly developed MCE-based sequential sampling approach [44], which will be employed later for efficient corrosion reliability analysis.

The MCE approach constructs surrogate models for system performances and updates these models based on a sequential sampling rule, so that accurate reliability estimations can be achieved using the MCS in an efficient manner. Let $\Omega_f = \{\mathbf{x} | G(\mathbf{x}, t) > 0\}$ denotes the failure region of a failure event for a given time t , thus the probability of failure can be computed in the MCS as

$$P_f = \Pr(\mathbf{x} \in \Omega_f) = \int_{\Omega_f} I_f(\mathbf{x}) f_{\mathbf{x}}(\mathbf{x}) d\mathbf{x} = E[I_f(\mathbf{x})] \quad (21)$$

where $\Pr(\cdot)$ represents a probability measure; $E[\cdot]$ denotes the expectation operator; and $I_f(\mathbf{x})$ is an indicator function and defined as

$$I_f(\mathbf{x}) = \begin{cases} 1, & \mathbf{x} \in \Omega_f \\ 0, & \text{otherwise} \end{cases} \quad (22)$$

According to Eq. (21), the probability of failure can be calculated using sampling methods such as MCS, although in general direct sampling is computationally prohibited due to a large number of function evaluations required. To reduce the computational cost of calculating the probability of failure using MCS, the Kriging technique [34,35] can be employed to develop a surrogate model, in which a performance function, $G(\mathbf{x}, t)$, is assumed to be generated by the surrogate model as

$$G(\mathbf{x}, t) = \mathbf{f}^T(\mathbf{x}, t)\boldsymbol{\alpha} + S(\mathbf{x}, t) \quad (23)$$

where $\mathbf{f}^T(\mathbf{x}, t) = [f_1(\mathbf{x}, t), \dots, f_b(\mathbf{x}, t)]$ is a basis function; $\boldsymbol{\alpha} = [\alpha_1, \dots, \alpha_b]$ is a regression coefficient vector; and $S(\mathbf{x}, t)$ is a Gaussian stochastic process at a given time t with zero mean and certain covariance matrix. The covariance function between two input \mathbf{x}_i and \mathbf{x}_j is expressed as

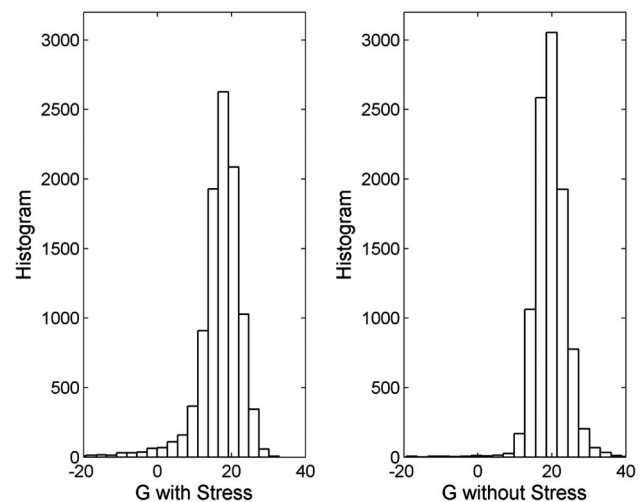


Fig. 4 Comparison of limit state functions with and without coupled stresses

$$\text{Cov}_{(i,j)} = \sigma^2 \mathbf{R}_{(i,j)} \quad (24)$$

where \mathbf{R} represents a correlation matrix. The (i, j) entry of matrix \mathbf{R} is described as

$$\mathbf{R}_{(i,j)} = \text{Corr}(\mathbf{x}_i, \mathbf{x}_j) = \exp \left[- \sum_{p=1}^k a_p |x_i^p - x_j^p|^{b_p} \right] \quad (25)$$

where Corr is a correlation function; a_p and b_p are parameters of the GP model; and k is the number of the input variables \mathbf{x} . With training observations, the response and predicted mean square error for any given new point \mathbf{x}' can be estimated by maximizing likelihood function [47] and expressed as

$$\hat{G}(\mathbf{x}') = \mu + \mathbf{r}^T \mathbf{R}^{-1} (\mathbf{G} - \mathbf{A}\mu) \quad (26)$$

$$\hat{\sigma}(\mathbf{x}') = \sigma^2 \left[1 - \mathbf{r}^T \mathbf{R}^{-1} \mathbf{r} + \frac{(1 - \mathbf{A}^T \mathbf{R}^{-1} \mathbf{r})^2}{\mathbf{A}^T \mathbf{R}^{-1} \mathbf{A}} \right] \quad (27)$$

where \mathbf{r} is the correlation vector between \mathbf{x}' and the observed samples.

In MCS, N random samples $\mathbf{X}_m = [\mathbf{x}_{m,1}, \dots, \mathbf{x}_{m,i}, \dots, \mathbf{x}_{m,N}]$ are generated according to the randomness of input in the sample space, then the reliability is calculated by

$$R = 1 - P_f = 1 - \frac{1}{N} \sum_{i=1}^N I_f(\mathbf{x}_{m,i}) \quad (28)$$

For the i th of MCS samples, $\mathbf{x}_m, \mathbf{x}_{m,i}$ can be bluntly classified as failure or safe. Due to the uncertainty of the GP model, the probability of correct classification for $\mathbf{x}_{m,i}$ can be obtained as

$$\text{POC}_i = \Phi \left(\frac{|\hat{G}(\mathbf{x}_{m,i})|}{\sqrt{\hat{\sigma}(\mathbf{x}_{m,i})}} \right) \quad (29)$$

where $|\cdot|$ is the absolute operator. Thus, the confidence of reliability approximation using MCS based on the GP model is obtained as

$$C_R = E[\text{POC}] = \frac{1}{N} \sum_{i=1}^N \text{POC}_i \quad (30)$$

The GP model should be updated by adding new samples if the confidence of reliability approximation is less than a confidence target. A new sample should be selected within MCS samples by maximizing the criterion defined as

$$C_S(\mathbf{x}_{m,i}) = (1 - \text{POC}_i) \times f_{\mathbf{X}}(\mathbf{x}_{m,i}) \times \sqrt{\hat{\sigma}(\mathbf{x}_{m,i})} \quad (31)$$

where POC_i is the probability of correct classification for $\mathbf{x}_{m,i}$ and $f_{\mathbf{X}}(\mathbf{x}_{m,i})$ is the probability density function value at $\mathbf{x}_{m,i}$; and $\hat{\sigma}(\mathbf{x}_{m,i})$ is the estimated mean square error. The updating process is employed and the reliability approximation is updated iteratively until the confidence of reliability approximation meets the confidence target.

Table 1 summarizes the procedure of the developed MCE-based adaptive sampling approach. To employ the MCE-based adaptive sampling method, starting from an initial sample set \mathbf{D} , an initial Kriging model \mathbf{M} can be built and the MCS can be employed with \mathbf{M} using N samples \mathbf{X}_m , then the reliability R and the CCL of reliability estimation $\text{CCL}(\mathbf{M}, \mathbf{X}_m)$ can be calculated using Eqs. (28) and (29), respectively. The estimated improvements $\text{EI}(\mathbf{X}_m)$ are computed for all the samples \mathbf{X}_m , and the sample \mathbf{x}^* with the largest estimated CCL improvement, $\text{Max}(\text{EI}(\mathbf{X}_m))$, will be selected as a new sample to update the Kriging model \mathbf{M} . This updating process is repeated until the termination rule is satisfied. Then the updated model \mathbf{M} will be used for reliability estimation. The Kriging model is considered to be a valid one if the CCL is greater than a confidence level target, CCL_T .

Table 1 Procedure of the MCE-based sequential sampling scheme

Steps	Procedure
Step 1	Identify initial data set \mathbf{D} ; initialize the confidence target CCL_T ; generate N samples \mathbf{X}_m according to the input randomness
Step 2	Develop a Kriging model \mathbf{M} using existing data set \mathbf{D}
Step 3	Compute the reliability R and confidence level $\text{CCL}(\mathbf{M}, \mathbf{X}_m)$
Step 4	Compare $\text{CCL}(\mathbf{M}, \mathbf{X}_m)$ with CCL_T : If $\text{CCL}(\mathbf{M}, \mathbf{X}_m) > \text{CCL}_T$, stop Otherwise, go to Step 5
Step 5	Compute $\text{EI}(\mathbf{X}_m)$ and obtain \mathbf{x}^* that has $\text{Max}(\text{EI}(\mathbf{X}_m))$. Evaluate $G(\mathbf{x}^*)$ and update \mathbf{D} by adding new data $(\mathbf{x}^*, G(\mathbf{x}^*))$; go to Step 2

Figure 5 shows the flowchart of employing the MCE-based adaptive sampling approach for corrosion reliability analysis using the developed corrosion model. As shown in the figure, the left-hand side shaded box details the MCE-based adaptive sampling approach, whereas the right-hand side shaded box explains the procedure of using the developed corrosion model for evaluating the performance function. For a given sample point \mathbf{x} , the MCE-based adaptive sampling approach on the right-hand side shaded box will execute the evaluation of the limit state function $G(\mathbf{x}, T)$ on the right-hand side shaded box at the given corrosion time T . Based on the developed corrosion model, the critical pit size will be computed based on the input sample \mathbf{x} , and the pit or crack size will continuously grow until the time t has reached beyond the defined corrosion time T . After the limit state function G is evaluated, the sample point, $(\mathbf{x}, G(\mathbf{x}, T))$, will be used to update the Kriging model. This process will be repeated until the target accuracy performance of the Kriging model is satisfied, and then the corrosion reliability will be calculated based on the developed Kriging model using the MCS method.

With the developed new corrosion model, and the MCE-based adaptive sampling method, the corrosion reliability can be estimated in an efficient manner. In the following section, a case study will be employed to demonstrate the efficacy of the proposed approach. The proposed approach will be compared with existing corrosion model without considering mechanical stress effects and the FORM.

5 Case Study for Corrosion Reliability Analysis

A case study is employed in this section to demonstrate the proposed physics-of-failure-based corrosion model and reliability analysis approach. The case study structure is idealized as an infinite plate with a pitting corrosion defect, while the pit corrosion occurs on the surface of the structure material, and the corrosive environment is assumed to be known. The structure material considered in this case study is the aluminum alloy, since it has been widely used in aerospace structures, energy engineering, and marine engineering applications. The uncertainties involved in material properties as well as the corrosion model parameters are considered and modeled with Gaussian random variables. The random and deterministic parameters used in this case study are listed in Tables 2 and 3, respectively [22,26]. As shown in Table 2, seven different random variables are employed in this case study, as specified by the mean values and standard deviations, where the standard deviations for all random variables have been taken as 5% of the given mean values. To demonstrate the proposed corrosion model at the pit-growth stage, considering the coupled effects of corrosion environment and the mechanical stresses, the corrosion time has been assumed to begin right after the pit nucleation, and without losing the generosity, the random pit nucleation has not considered in this example.

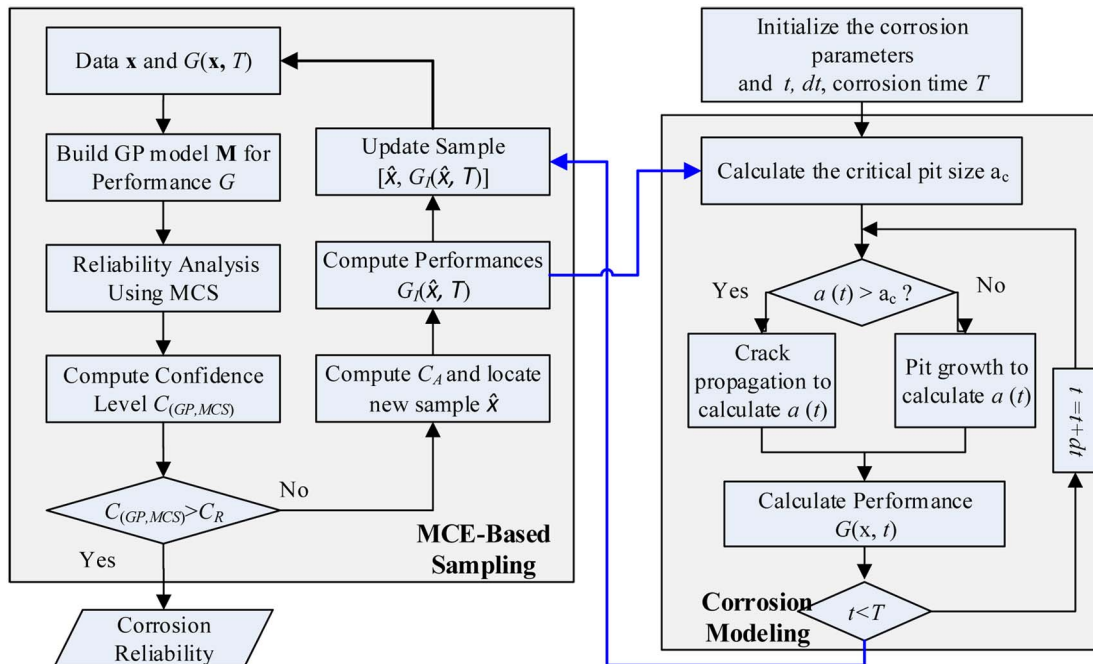


Fig. 5 Flowchart of reliability analysis with pitting corrosion damage

The structure reliability of pitting corrosion damage is calculated using MCS, FORM, and MCE-based adaptive sampling method. The MCS is used with a large number of samples ($N = 100,000$) as the benchmark solution to check the accuracy of the other two methods. The efficiency of the new MCE-based adaptive sampling approach is compared with the FORM based on the total times of the evaluations for the limit state function during the reliability analysis process.

First, the analysis of the limit state function and the corrosion failure probability assessment are conducted with three different approaches. Figure 4 in Sec. 3 shows the histograms of the limit state function value distribution at the corrosion time of 200 days with and without considering the coupled mechanical stress effects, respectively. From the figure, it is clear that ignoring the coupled stress effect, an underestimated failure probability value will be very much likely obtained, and the developed pit-growth model that considers the coupled stress effect can effectively overcome this

deficiency of the existing model. Figure 6 provides 100 random realizations of the pit-growth curve over time considering the random inputs as shown in Table 2. It is clear from the figure that the random inputs yield a large deviation for the pit-growth curve over time. With the random variables shown in Table 2, the corrosion reliability analysis is then carried out with different corrosion times using three different approaches as mentioned earlier, and the analysis results are summarized in Tables 4 and 5. From the results comparison in Table 4, the probability of failure estimations with MCE-based adaptive sampling method turn out to be more accurate consistent, as indicated by the percentage errors, than those obtained by FORM, compared with the results obtained by MCS with a sample size of 10^5 . The comparison of the probability of failure estimations and the absolute percentage errors obtained using the MCE-based adaptive sampling method, the FORM method compared with the MCS results are also shown in Figs. 7 and 8, respectively. It is clear from the figures that the MCE-based adaptive

Table 2 Random variables for case study

Random variables	Unit	Mean	STD (Mean%)
a_0	m	1.98×10^6	10%
I_0	c/s	6.5×10^6	10%
K_{IC}	MPa/m ²	35	10%
σ_s	MPa	470	10%
$\Delta\sigma$	MPa	90	10%
C	–	2.8×10^{11}	10%
m	–	1.16	10%

Table 3 Deterministic model parameters for the case study

Variables	Value	Variable	Value
k_r	2.6	z	3
α	1.15	ρ	2.7×10^6 g/m ³
η	0.12 V	F	96,514 C/mol
β	2.6	ΔH	50 kJ/mol
M	27 g/mol	T	293 K
R	8.314 J/mol K	V_m	10 cm ³ /mol

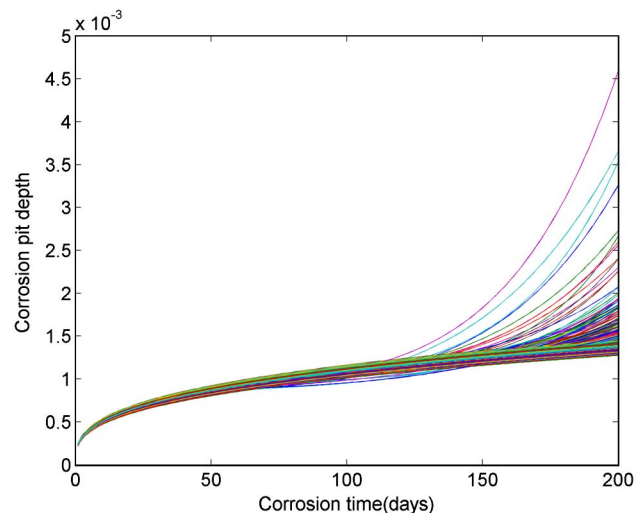


Fig. 6 Pit depth growth curve with different corrosion time

Table 4 Analysis results with different corrosion times

Corrosion time (day)	Probability of failure				
	MCS	MCE	MCE error (%)	FORM	FORM error (%)
250	0.00185	0.00267	44.32432	0.00132	28.64865
300	0.00887	0.00780	12.06313	0.00504	43.17926
350	0.02964	0.02975	0.37112	0.01703	42.54386
400	0.06605	0.06132	7.16124	0.04628	29.93187
450	0.11926	0.12059	1.11521	0.09411	21.08838
500	0.18524	0.18250	1.47916	0.15888	14.23019

Table 5 Comparison of efficiency between MCE and FORM

Corrosion time	MCE			FORM
	Number of initial samples	Number of samples for GP updating	Number of total samples	
250	28	26	54	800
300	28	18	46	800
350	28	33	61	136
400	28	42	70	232
450	28	50	78	288
500	28	60	88	128

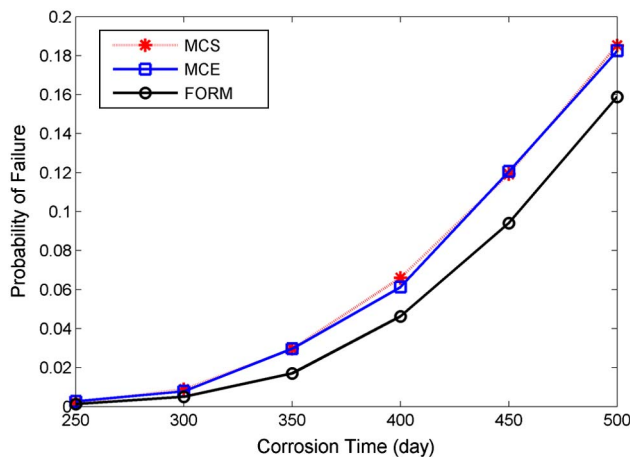


Fig. 7 Probability of failure analysis results at different corrosion times

sampling method provides a constantly higher accuracy than the FORM for corrosion failure probability analysis, especially with the undergoing corrosion time gets longer. Besides the accuracy performance, the efficiencies of corrosion failure probability analysis using the MCE-based adaptive sampling method and the FORM are also compared, as the results shown in Table 5, in which the number of sample points being evaluated for the limit state function is employed as the accuracy measure. For the MCE-based adaptive sampling method, the initial samples used to build the Kriging model are set to 28, and the samples are also used to update the Kriging model adaptively to improve its accuracy. Thus, the total sample points used for the MCE method are the summation of the initial samples and the updating samples. As shown in the last two columns in the table, the FORM generally requires more sample points to be evaluated to conduct reliability analysis, compared with the MCE-based method. Moreover, due to the gradient-based searching process employed by the FORM to find the MPP, the gradient information must be provided, which in this study the finite difference method has been employed for the FORM to provide the

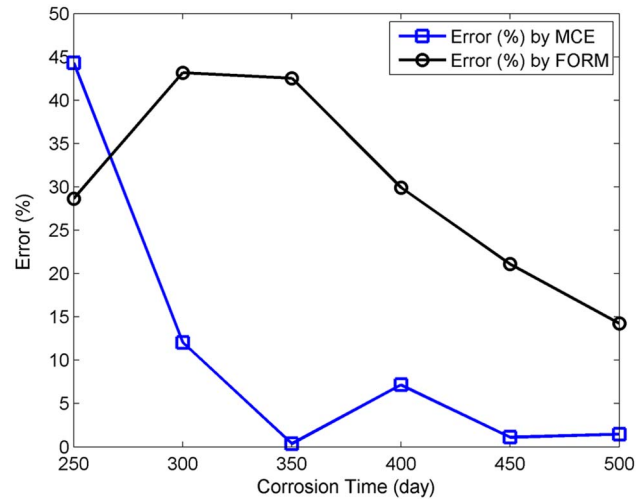


Fig. 8 Errors of failure probability analysis at different corrosion times

required information. As the gradient-based method is used for MPP search, the searching process may not converge to the true MPP efficiently in some scenarios, as shown in the table for corrosion time of 250 days and 300 days in which the total numbers of sample evaluations for both have reached the upper limit of 800.

From the case study results, it is clear that the unique advantages of the MCE-based adaptive sampling approach for corrosion reliability analysis are from two facets: (1) due to the adaptive nature of the MCE-based approach, it is able to efficiently sample necessary failure points for the accuracy improvement of the reliability analysis, thus to the maximum extent enhancing the computational efficiency while maintaining a given accuracy requirement and (2) the confidence measure employed for sampling enables the control of the accuracy in corrosion reliability analysis based on the user needs. Given that the corrosion reliability analysis involves corrosion time in the limit state function, evaluating the limit state functions over time becomes very computationally expensive. Employing the MCE-based adaptive sampling approach can substantially improve the efficiency and accuracy, as demonstrated from the case study results.

6 Conclusions

A new physics-of-failure model for pitting corrosion considering the coupled effect of corrosion environment and mechanical stresses has been developed in this paper. With the developed model, corrosion damage growth can be projected thereby corrosion failure probability can be conveniently analyzed. It is shown that considering the coupled effect of corrosion environment with mechanical stresses, the corrosion reliability tends to be much lower compared with existing corrosion models that ignore this coupled effect. To carry out corrosion reliability analysis, the developed pitting corrosion model can be formulated as time-dependent limit state functions considering pit to crack transition, crack growth, and fracture failure mechanics. An MCE-based sequential approach has been employed to improve the accuracy and efficiency of corrosion reliability analysis with the time-dependent limit state functions. A case study has been used to demonstrate the efficacy of the developed physics-of-failure model for corrosion considering the coupled mechanical stress effects together with the new corrosion reliability analysis methodology. The performance of corrosion reliability analysis employing the new MCE-based adaptive sampling approach has been compared with the existing FORM approach, and the results have shown that the new approach outperforms the FORM approach on reliability estimation accuracy and efficiency.

Future work can be done to apply the developed physics-of-failure model for structure corrosion failure predication and corrosion life estimation.

Acknowledgment

This research was partially supported by National Science Foundation through Faculty Early Career Development (CAREER) award under Grant No. CMMI-1351414, the Foundation of China Academic Engineering Physics (CAEP) under Grant No. 2013B0203028, the Technology Foundation Project under Grant No. 2013ZK1.2, and the NSAF under Grant No. U1330130.

References

- [1] Melchers, R. E., 2005, "The Effect of Corrosion on the Structural Reliability of Steel Offshore Structures," *Corros. Sci.*, **47**(10), pp. 2391–2410.
- [2] Hoepfner, D. W., and Arriscorreta, C. A., 2012, "Exfoliation Corrosion and Pitting Corrosion and Their Role in Fatigue Predictive Modeling: State-of-the-Art Review," *Int. J. Aerosp. Eng.*, **2012**, p. 29.
- [3] Yokobori, A. T., 2004, "The Mechanism of Hydrogen Embrittlement: The Stress Interaction Between a Crack, a Hydrogen Cluster, and Moving Dislocations," *Int. J. Fract.*, **128**, pp. 121–131.
- [4] Elboudjaini, M., and Revie, R. W., 2009, "Metallurgical Factors in Stress Corrosion Cracking and Hydrogen-Induced Cracking," *J. Solid State Electrochem.*, **13**(7), pp. 1091–1099.
- [5] Teixeira, A. P., Guedes Soares, C., Netto, T. A., and Estefen, S. F., 2008, "Reliability of Pipelines With Corrosion Defects," *Int. J. Press. Vessels Pip.*, **85**(4), pp. 228–237.
- [6] Anoop, M. B., Rao, K. B., and Lakshmana, N., 2008, "Safety Assessment of Austenitic Steel Nuclear Power Plant Pipelines Against Stress Corrosion Cracking in the Presence of Hybrid Uncertainties," *Int. J. Press. Vessels Pip.*, **85**(4), pp. 238–247.
- [7] Li, S., Yu, S., Zeng, H., Li, J., and Liang, R., 2009, "Predicting Corrosion Remaining Life of Underground Pipelines With a Mechanically-Based Probabilistic Model," *J. Pet. Sci. Eng.*, **65**(3–4), pp. 162–166.
- [8] Qian, G., Niffenegger, M., and Li, S., 2011, "Probabilistic Analysis of Pipelines With Corrosion Defects by Using FITNET FFS Procedure," *Corros. Sci.*, **53**(3), pp. 855–861.
- [9] Nuhli, M., Seer, T. A., Tamini, A. M., Modarres, M., and Seibi, A., 2011, "Reliability Analysis for Degradation Effects of Pitting Corrosion in Carbon Steel Pipes," *Proc. Eng.*, **10**, pp. 1930–1935.
- [10] Paik, J. K., Kim, S. K., and Lee, S. K., 1998, "Probabilistic Corrosion Rate Estimation Model for Longitudinal Strength Members of Bulk Carriers," *Ocean Eng.*, **25**(10), pp. 837–860.
- [11] Melchers, R. E., 1999, "Corrosion Uncertainty Modeling for Steel Structures," *J. Constr. Steel Res.*, **52**(1), pp. 3–19.
- [12] Qin, S. P., and Cui, W., 2003, "Effect of Corrosion Model on the Time-Dependent Reliability of Steel Plated Elements," *Mar. Struct.*, **16**(1), pp. 15–34.
- [13] Melchers, R. E., 2005, "Representation of Uncertainty in Maximum Depth of Marine Corrosion Pits," *Struct. Saf.*, **27**(4), pp. 322–334.
- [14] Yu, S., Jieze, Y., and Tingchao, Y., 2010, "Mechanical Model and Probability Analysis of Buried Pipelines Failure Under Uniform Corrosion," *J. Zhejiang Univ.*, **44**(6), pp. 1125–1230.
- [15] Engelhardt, G., and Macdonalds, D. D., 2004, "Unification of the Deterministic and Statistical Approaches for Predicting Localized Corrosion Damage. I. Theoretical Foundation," *Corros. Sci.*, **46**(11), pp. 2755–2780.
- [16] Sheikh, A. K., Boah, J. K., and Hansen, D. A., 1990, "Statistical Modeling of Pitting Corrosion and Pipeline Reliability," *Corros. Sci.*, **46**(3), pp. 190–197.
- [17] Caleyó, F., and Velazquez, J. C., 2009, "Markov Chain Modelling of Pitting Corrosion in Underground Pipelines," *Corros. Sci.*, **51**(9), pp. 2197–2207.
- [18] Valor, A., Caleyó, F., and Alfonso, L., 2007, "Stochastic Modeling of Pitting Corrosion: A New Model for Initiation and Growth of Multiple Corrosion Pits," *Corros. Sci.*, **49**(2), pp. 559–579.
- [19] Zhang, T., Liu, X., Shao, Y., Meng, G., and Wang, F., 2008, "Electrochemical Noise Analysis on the Pit Corrosion Susceptibility of Mg-10Gd-2Y-0.5Zr, AZ91D Alloy and Pure Magnesium Using Stochastic Model," *Corros. Sci.*, **50**(12), pp. 3500–3507.
- [20] Xu, L. Y., and Cheng, Y. F., 2012, "Reliability and Failure Pressure Prediction of Various Grades of Pipeline Steel in the Presence of Corrosion Defects and Pre-Strain," *Int. J. Press. Vessels Pip.*, **89**, pp. 75–84.
- [21] Harlow, D. G., and Wei, R. P., 1994, "Probability Approach for Prediction of Corrosion and Corrosion Fatigue Life," *AIAA J.*, **32**(10), pp. 2073–2079.
- [22] Shi, P., and Mahadevan, M., 2001, "Damage Tolerance Approach for Probabilistic Pitting Corrosion Fatigue Life Prediction," *Eng. Fract. Mech.*, **68**(13), pp. 1493–1507.
- [23] Wu, G., 2011, "A Probabilistic-Mechanistic Approach to Modeling Stress Corrosion Cracking Propagation in Alloy 600 Components With Applications," Ms.D. Dissertation, University of Maryland.
- [24] Kondo, Y., 1989, "Prediction of Fatigue Crack Initiation Life Based on Pit Growth," *Corrosion*, **45**(1), pp. 7–11.
- [25] Bedairi, B., Cronin, D., Hosseini, A., and Plumtree, A., 2012, "Failure Prediction for Crack-In-Corrosion Defects in Natural Gas Transmission Pipelines," *Int. J. Press. Vessels Pip.*, **96**–97, pp. 90–99.
- [26] Harlow, D. G., and Wei, R. P., 1998, "A Probability Model for the Growth of Corrosion Pits in Aluminum Alloys Induced by Constituent Particles," *Eng. Fract. Mech.*, **53**(3), pp. 205–325.
- [27] Helton, J. C., and Davis, F. J., 2003, "Latin Hypercube Sampling and the Propagation of Uncertainty in Analyses of Complex Systems," *Reliab. Eng. Syst. Saf.*, **81**(1), pp. 23–69.
- [28] Hasofer, A. M., and Lind, N. C., 1974, "Exact and Invariant Second-Moment Code Format," *J. Eng. Mech. Div. ASCE*, **100**(1), pp. 111–121.
- [29] Tvedt, L., 1984, "Two Second-Order Approximations to the Failure Probability," *Section on Structural Reliability, A/S Vertas Research, Hovik*.
- [30] Wang, L. P., and Grandhi, R. V., 1996, "Safety Index Calculation Using Intervening Variables for Structural Reliability," *Comput. Struct.*, **59**(6), pp. 1139–1148.
- [31] Au, S. K., and Beck, J. L., 2001, "Estimation of Small Failure Probabilities in High Dimensions by Subset Simulation," *Probab. Eng. Mech.*, **16**(4), pp. 263–277.
- [32] Englund, S., and Rackwitz, R., 1993, "A Benchmark Study on Importance Sampling Techniques in Structural Reliability," *Struct. Saf.*, **12**(4), pp. 255–276.
- [33] Rahman, S., and Xu, H. A., 2004, "A Univariate Dimension-Reduction Method for Multi-Dimensional Integration in Stochastic Mechanics," *Probab. Eng. Mech.*, **19**(4), pp. 393–408.
- [34] Lee, I., Choi, K. K., Du, L., and Gorsich, D., 2008, "Dimension Reduction Method for Reliability-Based Robust Design Optimization," *Spec. Issue Comput. Struct.: Struct. Multidiscip. Optim.*, **86**(13–14), pp. 1550–1562.
- [35] Xu, H., and Rahman, S., 2004, "A Generalized Dimension-Reduction Method for Multidimensional Integration in Stochastic Mechanics," *Int. J. Numer. Method Eng.*, **61**(12), pp. 1992–2019.
- [36] Ghanem, R. G., and Spanos, P. D., 1991, *Stochastic Finite Elements: A Spectral Approach*, Springer, New York.
- [37] Paffrath, M., and Wever, U., 2007, "Adapted Polynomial Chaos Expansion for Failure Detection," *J. Comput. Phys.*, **226**, pp. 263–281.
- [38] Xiu, D., and Karniadakis, G. E., 2003, "The Wiener-Askey Polynomial Chaos for Stochastic Differential Equations," *SIAM J. Sci. Comput.*, **18**(2), pp. 137–167.
- [39] Simpson, T. W., Mauery, T. M., Korte, J. J., and Mistree, F., 1998, "Comparison of Response Surface and Kriging Models for Multidisciplinary Design Optimization," 7th AIAA/USAF/NASA/ISSMO Symposium on Multidisciplinary Analysis and Optimization, AIAA Paper No. AIAA-98-4755.
- [40] Xiong, Y., Chen, W., and Tsui, K., 2008, "A New Variable Fidelity Optimization Framework Based on Model Fusion and Objective-Oriented Sequential Sampling," *J. Mech. Des.*, **130**(11), p. 111401.
- [41] Queipo, N. V., Haftka, R. T., Shyy, W., Goel, T., Vaidyanathan, R., and Tucker, P. K., 2005, "Surrogate-Based Analysis and Optimization," *Prog. Aerosp. Sci.*, **41**(1), pp. 1–28.
- [42] Gu, L., Yang, R. J., Tho, C. H., Makowskit, M., Faruquet, O., and Li, Y., 2001, "Optimization and Robustness for Crashworthiness of Side Impact," *Int. J. Veh. Des.*, **26**(4), pp. 348–360.
- [43] Zhao, L., Choi, K. K., and Lee, I., 2011, "Metamodeling Method Using Dynamic Kriging for Design Optimization," *AIAA J.*, **49**(9), pp. 2034–2046.
- [44] Wang, Z., and Wang, P., 2012, "A Nested Extreme Response Surface Approach for Time-Dependent Reliability-Based Design Optimization," *ASME J. Mech. Des.*, **134**(12), p. 121007.
- [45] Wang, Z., and Wang, P., 2012, "A Maximum Confidence Enhancement Based Sequential Sampling Scheme for Simulation-Based Design," *ASME J. Mech. Des.*, **136**(14), pp. 021006.
- [46] Aloseyabi, M. C., 2009, "Structuring a Probabilistic Model for Reliability Evaluation of Piping Subject to Corrosion-Fatigue Degradation," Ph.D. Dissertation, University of Maryland.
- [47] Gutman, E. M., 1994, *Mechanochemistry of Solid Surfaces*, World Scientific Publications, Singapore.
- [48] Jiang, X., Chu, W., and Xiao, J., 1995, "Fractal Analysis of Orientation Effect on K_{IC} and K_{ISCC} ," *Eng. Fract. Mech.*, **51**(5), pp. 805–808.
- [49] Shin, K. I., Park, J. H., Kim, H.-D., and Chung, H.-S., 2002, "Simulation of Stress Corrosion Crack Growth in Steam Generator Tubes," *Nucl. Eng. Des.*, **214**(1–2), pp. 91–101.
- [50] Yang, Y., and Zhang, T., 2013, "New Understanding of the Effect of Hydrostatic Pressure on the Corrosion of Ni-Cr-Mo-V High Strength Steel," *Corros. Sci.*, **73**, pp. 250–261.
- [51] Xu, L. Y., and Cheng, F. Y., 2013, "Development of a Finite Element Model for Simulation and Prediction of Mechanoelectrochemical Effect of Pipeline Corrosion," *Corros. Sci.*, **73**, pp. 150–160.